Rapid Communications

Obtaining Majorana and other boundary modes from the metamorphosis of impurity-induced states: Exact solutions via the T-matrix

Vardan Kaladzhyan[1,*] and Cristina Bena[2]

[1]*Department of Physics, KTH Royal Institute of Technology, SE-106 91 Stockholm, Sweden*

[2]*Institut de Physique Théorique, Université Paris Saclay, CEA CNRS, Orme des Merisiers, F-91190 Gif-sur-Yvette Cedex, France*

(Received 20 November 2018; published 12 August 2019)

We provide here a direct and exact formalism to describe the formation of edge or surface states, as well as to calculate boundary Green's functions. Modeling the boundary as an impurity potential, we show via the T-matrix formalism that the impurity states evolve into boundary modes when the impurity potential goes to infinity. We apply this technique to obtain Majorana states in one- (1D) and two-dimensional Kitaev systems. For the 1D case we also calculate the corresponding boundary Green's functions. We argue that our formalism can be applied to other topological models, as well as to any model exhibiting edge states.

DOI: 10.1103/PhysRevB.100.081106

Introduction. One of the oldest and challenging quantum physics problems is taking into account the presence of boundaries. As Pauli once said, "God made the bulk; surfaces were invented by the devil" [1]. One of the most common techniques to describe the boundary effects is the numerical diagonalization of a tight-binding Hamiltonian [2,3]. Analytically, the formation of boundary modes is usually studied by solving the Schrödinger equation with specific boundary conditions [4]. The latter is sometimes cumbersome and oftentimes requires making specific approximations which decrease the generality of the solution. Less common techniques rely on the use of boundary Green's functions [5–7] and the bulk-boundary correspondence [8].

Here, we propose a general, direct, and exact technique to obtain the energies and the wave functions of boundary modes in systems of arbitrary dimensions. Instead of solving the problem of a finite-size system with a desired boundary, we suggest to consider an infinite system with a localized impurity. We subsequently obtain the corresponding impurity-induced states using the T-matrix formalism [9]. As intuitively expected, we show that by taking the impurity potential to infinity we recover the formation of edge states. Remarkably, this technique also allows us to obtain in a very simple and straightforward manner the boundary Green's functions, while previous derivations of such quantities are often not exact and harder to implement.

For the sake of clarity, we exemplify our proposal by focusing on the formation of Majorana end modes in a Kitaev chain [10] and Majorana chiral edge states in a two-dimensional (2D) p-wave superconductor [11–13]. We also calculate the boundary Green's function for the former and compare the result with previous calculations [7]. Moreover, we show that the analytical T-matrix formalism is entirely consistent with a numerical tight-binding calculation.

We thus suggest the following algorithm for finding edge states:

(1) Take an infinite 1D, 2D, or 3D system.

(2) Introduce a point, line, or plane scalar impurity described by a delta-function potential (see Fig. 1).

(3) Use the T-matrix formalism to find the Green's functions for the perturbed system, as well as the energies and wave functions of the impurity-bound states.

(4) Formally set the impurity potential to infinity to recover the formation of boundary modes and the boundary Green's functions.

T-matrix formalism. We denote the momentum-space Hamiltonian of a given system $\mathcal{H}_{\boldsymbol{p}}$, and we define the unperturbed Matsubara Green's function (GF) as follows, $G_0(\boldsymbol{p}, i\omega_n) \equiv (i\omega_n - \mathcal{H}_{\boldsymbol{p}})^{-1}$, where ω_n denote Matsubara frequencies. In the presence of an impurity $V_{\text{imp}}(\boldsymbol{r})$ the latter is modified to

$$G(\boldsymbol{p}_1, \boldsymbol{p}_2, i\omega_n) = G_0(\boldsymbol{p}_1, i\omega_n)\delta(\boldsymbol{p}_1 - \boldsymbol{p}_2) + G_0(\boldsymbol{p}_1, i\omega_n)T(\boldsymbol{p}_1, \boldsymbol{p}_2, i\omega_n)G_0(\boldsymbol{p}_2, i\omega_n), \tag{1}$$

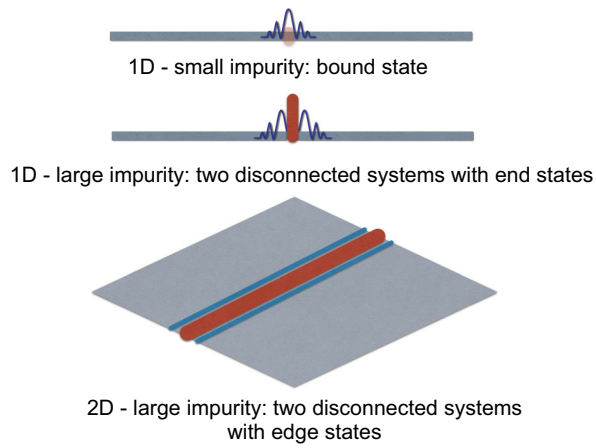

FIG. 1. A simple exemplification of a 1D system with a localized impurity: When the impurity potential goes to infinity, this is equivalent to two disconnected semi-infinite wires. Similarly, a 2D infinite system with a linelike infinite-potential impurity is equivalent to two disconnected half planes.

*vardan.kaladzhyan@phystech.edu

where the T-matrix $T(\boldsymbol{p}_1, \boldsymbol{p}_2, i\omega_n)$ describes the cumulated effect of all-order impurity-scattering processes [9,14]. For the particular case of a delta-function impurity $V_{\text{imp}}(\boldsymbol{r}) = V\delta(x)$, the form of the T-matrix in 1D is momentum independent and is given by [9,15–18]

$$T(i\omega_n) = \left[\mathbb{I} - V \cdot \int \frac{dp}{2\pi} G_0(p, i\omega_n)\right]^{-1} \cdot V, \tag{2}$$

while in 2D we have

$$T(p_{1x}, p_{1y}, p_{2x}, p_{2y}, i\omega_n) = \delta(p_{1y} - p_{2y})\left[\mathbb{I} - V \cdot \int \frac{dp_x}{2\pi} G_0(p_x, p_{1y}, i\omega_n)\right]^{-1} \cdot V. \tag{3}$$

Note that this is independent of p_{1x} and p_{2x} (due to the fact the impurity is a delta potential in the x direction, and conversely, that it is a delta function in $p_{1y} - p_{2y}$ since the impurity is independent of position in the y direction). When $V \to \infty$, $G(\boldsymbol{p}_1, \boldsymbol{p}_2, i\omega_n)$ the corresponding Fourier transforms become the boundary GFs, and the poles of the T-matrix yield the energies of the edge states.

In what follows we use this formalism at zero temperature to calculate the retarded GF $\mathcal{G}(\boldsymbol{p}_1, \boldsymbol{p}_2, E)$ obtained by the analytical continuation of the Matsubara GF $G(\boldsymbol{p}_1, \boldsymbol{p}_2, i\omega_n)$ (i.e., by setting $i\omega_n \to E + i\delta$, with $\delta \to +0$).

1D Kitaev chain. We start by considering an infinite spinless Kitaev chain described by the Hamiltonian

$$\mathcal{H}_{\text{TB}} = \sum_i -\mu c_i^\dagger c_i - (t c_i^\dagger c_{i+1} - \Delta c_i c_{i+1} + \text{H.c.}), \tag{4}$$

where $c_i^\dagger$ (c_i) are creating (annihilating) operators on the ith site, t is the hopping amplitude, μ denotes the chemical potential, and $\Delta > 0$ is the superconducting pairing amplitude. We set the lattice constant a as well as $\hbar$ to unity. In momentum space the Hamiltonian in Eq. (4) becomes

$$\mathcal{H}_p^{\text{1D}} = \begin{pmatrix} -\mu/2 - t\cos p & i\Delta \sin p \\ -i\Delta \sin p & \mu/2 + t\cos p \end{pmatrix}. \tag{5}$$

We introduce an impurity into the chain, localized at $x = 0$,

$$V_{\text{imp}}(x) = U\delta(x)\begin{pmatrix} 1 & 0 \\ 0 & -1 \end{pmatrix} \equiv U\delta(x)\tau_z. \tag{6}$$

We solve the problem of the impurity Yu-Shiba-Rusinov (YSR) states [19–21] exactly using the T-matrix formalism described above (see also Refs. [22–24]). In momentum space the unperturbed retarded GF is given by $\mathcal{G}_0(p, E) = [E + i0 - \mathcal{H}_p^{\text{1D}}]^{-1}$, and the corresponding real-space GF $\mathcal{G}_0(x, E) = \int \frac{dp}{2\pi} \mathcal{G}_0(p, E) e^{ipx}$. We take $\mu = 0$ and we compute analytically the real-space GF at $x = 0$,

$$\mathcal{G}_0(0, E) = \begin{pmatrix} EX_0(0) & 0 \\ 0 & EX_0(0) \end{pmatrix}, \tag{7}$$

with $X_0(0) = -(\sqrt{t^2 - E^2}\sqrt{\Delta^2 - E^2})^{-1}$. The energies of the impurity bound states can be obtained by calculating the poles of the T-matrix,

$$1 \pm U \frac{1}{\sqrt{t^2 - E^2}} \frac{E}{\sqrt{\Delta^2 - E^2}} = 0. \tag{8}$$

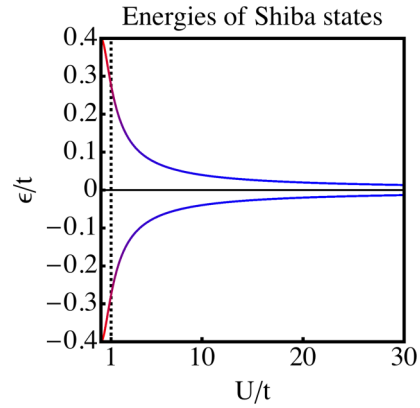

FIG. 2. The energies of YSR states given by Eq. (9) plotted as a function of the impurity strength U (in units of t). The black dashed line corresponds to $U/t = 1$, for which $E/t \approx 0.28$. The energies asymptotically approach zero when $U \to \infty$ marking the metamorphosis of YSR states into Majorana states. We have set $\mu/t = 0$, $\Delta/t = 0.4$.

This equation yields a pair of spurious solutions outside the gap, and a pair of YSR-like solutions inside the gap,

$$E_\pm = \pm\sqrt{\frac{1}{2}[t^2 + \Delta^2 + U^2 - \sqrt{(t^2 + \Delta^2 + U^2)^2 - 4t^2\Delta^2}]}. \tag{9}$$

When $U \to 0$ these solutions approach the edges of the gap, i.e., $E_\pm \to \pm\Delta$ (see Fig. 2), whereas when $U \to \infty$ these solutions decay as

$$E_\pm = \pm\frac{\Delta}{U/t}. \tag{10}$$

We can also obtain the impurity wave functions using Refs. [22–24],

$$\Psi(x) \propto \mathcal{G}_0(x, E) \cdot \tau_z \cdot \Psi(0),$$

where $\Psi(0) = (1\ 0)^{\text{T}}$ (for $E = E_+$) and $\Psi(0) = (0\ 1)^{\text{T}}$ (for $E = E_-$) are the null-space vectors of the matrix $\mathbb{I}_2 - U\tau_z \cdot \mathcal{G}_0(0, E)$.

In the case of an infinite potential the energies of the bound states $E_\pm \to \pm 0$. In what follows we consider that x can only be an integer multiple of the lattice constant a, i.e., $x = na$, with $n \in \mathbb{Z}$. This is a fair restriction taking into account that we work within a lattice model. This allows us to obtain an exact form for the two zero-energy wave functions,

$$\Psi_1(x) \propto \begin{pmatrix} 1 \\ -\operatorname{sgn} x \end{pmatrix} e^{-\frac{1}{2}\ln\left(\frac{1+\Delta/t}{1-\Delta/t}\right)|x|} \sin\left(\frac{\pi|x|}{2}\right), \tag{11}$$

$$\Psi_2(x) \propto \begin{pmatrix} -\operatorname{sgn} x \\ 1 \end{pmatrix} e^{-\frac{1}{2}\ln\left(\frac{1+\Delta/t}{1-\Delta/t}\right)|x|} \sin\left(\frac{\pi|x|}{2}\right). \tag{12}$$

We note that by combining states 1 and 2 we get left and right Majorana bound states, since the factors $\frac{1\pm\operatorname{sgn} x}{2}$ ensure that the WF "lives" either only on the left side or on the right side of the impurity. The Majorana coherence length is given by $\xi = [\frac{1}{2}\ln(\frac{1+\Delta/t}{1-\Delta/t})]^{-1}$, and diverges as t/Δ when $\Delta \to 0$. Such behavior is expected since the Majorana bound states become more and more delocalized when reducing Δ. Note that the

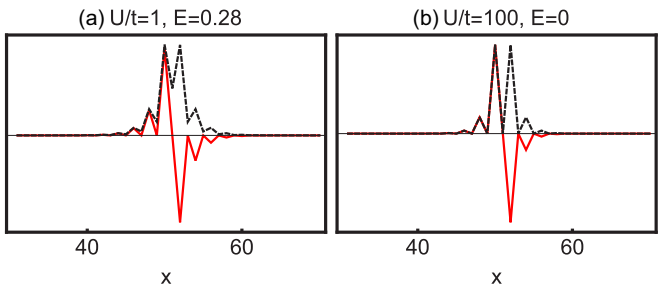

FIG. 3. The local DOS (black dashed lines) and the Majorana polarization (red solid lines) plotted as a function of position for $U/t = 1$, $E/t \approx 0.28$ (left panel), and $U/t = 100$, $E/t \approx 0$ (right panel). YSR states form for an impurity strength $U/t = 1$, whereas for $U/t = 100$ they morph into Majorana states localized on the two sides of the potential barrier at $x = 51$. We have considered a chain of 101 sites and we have set $\mu/t = 0$, $\Delta/t = 0.4$.

wave functions in Eqs. (11) and (12) fully correspond to those calculated in Ref. [10].

We confirm these findings numerically by diagonalizing a 1D Kitaev chain with an impurity using the MATQ code [25], and by plotting the Majorana polarization (red line) and the local density of states (DOS) (black dashed line) for the impurity-bound states (see Fig. 3). The energy of the impurity-bound states goes to zero with increasing the impurity strength, for instance, we get $E \approx 0.28$ and $E \approx 0$ when setting $U/t = 1$ and $U/t = 100$, respectively (the other parameters are $\mu/t = 0$ and $\Delta/t = 0.4$). The Majorana polarization [26,27] differs from the density of states (DOS) for small impurity strengths [see Fig. 3(a)], but they become equal (up to a sign) when the impurity potential goes to infinity [Fig. 3(b)]. This indicates [26,27] the formation of Majorana states at the ends of the two systems obtained by cutting the original system into two disconnected halves. Note the perfect agreement between the numerical and the analytical techniques: the one-to-one correspondence for the energies of the bound states between Figs. 2, 3, and Eq. (9), as well as for the form of the wave functions in Eqs. (11) and (12) versus Fig. 3.

We also discuss the versatility of our method in terms of obtaining the boundary GFs of a system. This can be done easily, directly, and exactly by noting that $\mathcal{G}_b \equiv \mathcal{G}_0 + \mathcal{G}_0 T_\infty \mathcal{G}_0$, with the exact form of $\mathcal{G}_0$ given in Eq. (7). For $\mu = 0$, T_∞ is given by

$$T_\infty(E + i0) = \lim_{U\to\infty} [\mathbb{I} - U\tau_z \mathcal{G}_0(0, E + i0)]^{-1} U\tau_z$$
$$= -[\mathcal{G}_0(0, E + i0)]^{-1} = \frac{\sqrt{t^2 - E^2}\sqrt{\Delta^2 - E^2}}{E + i0}\tau_0.$$

We can compare our result with the approach in Ref. [7] where the authors proposed to use a recurrent procedure to derive the boundary GF for a Kitaev chain. They find that in the topological regime it has a pole at $E = 0$, consistent with the formation of MBS. This is what transpires also from our expressions above corresponding to $\mu = 0$. In order to capture the transitions to a trivial phase at $\mu = \pm 2t$ we study the dependence of the boundary GF (or equivalently of the T-matrix) on μ. We find that such a phase transition

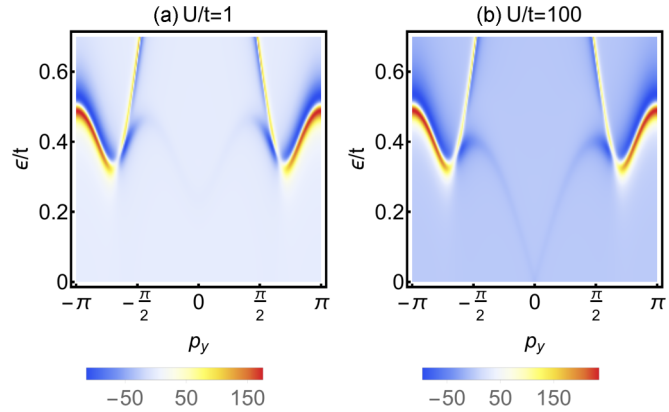

FIG. 4. On the left (right) panel we present the average spectral function of a 2D infinite system in the presence of a weak (strong) linelike impurity, plotted as a function of p_y. For a weak impurity we take $U/t = 1$ and we see clearly the formation of a subgap Shiba band, which for a strong impurity with $U/t = 100$ morphs into chiral dispersive Majorana modes with energies $E_\pm = \pm\varkappa p_y$. We have set $\mu/t = 0.5$, $\varkappa/t = 0.4$, and the quasiparticle broadening $\delta/t = 0.03$.

is captured perfectly: In the topological regime the T-matrix has a pole at $E = 0$, whereas in the trivial one its behavior is regular. This result is in perfect agreement with the results of Ref. [7]. For brevity, we leave this demonstration to the Supplemental Material [28]. Moreover, we should stress once more the simplicity and the directness of our approach, as well as the absence of any approximation or supplementary assumption.

2D p-wave superconductor. Below we turn to an infinite 2D system with a deltalike line impurity at $x = 0$ described by the real-space tight-binding Hamiltonian

$$\mathcal{H}_{\rm TB}^{\rm 2D} = \sum_{m,n} -\mu c_{m,n}^\dagger c_{m,n} - [t(c_{m+1,n}^\dagger c_{m,n} + c_{m,n+1}^\dagger c_{m,n})$$
$$- \Delta(c_{m,n}c_{m+1,n} - i\, c_{m,n}c_{m,n+1}) + \text{H.c.}], \qquad (13)$$

where μ denotes the chemical potential, t is the hopping parameter, and $\Delta > 0$ is the pairing amplitude. Operators $c_{m,n}^\dagger(c_{m,n})$ create (annihilate) spinless fermions on the site (m, n). The corresponding momentum-space Hamiltonian is

$$\mathcal{H}_{\boldsymbol{p}}^{\rm 2D} = \begin{pmatrix} \epsilon_{\boldsymbol{p}} & \Delta_{\boldsymbol{p}} \\ \Delta_{\boldsymbol{p}}^* & -\epsilon_{\boldsymbol{p}} \end{pmatrix}, \qquad (14)$$

with $\epsilon_{\boldsymbol{p}} \equiv -\mu/2 - t(\cos p_x + \cos p_y)$, $\Delta_{\boldsymbol{p}} = i\Delta(\sin p_x + i \sin p_y)$.

The line impurity can be described by Eq. (6). From Eq. (3) we see that the poles of the T-matrix, which correspond to the impurity energy levels, are p_y dependent and can be obtained by solving

$$\det\left[\mathbb{I}_2 - U\tau_z \cdot \int \frac{dp_x}{2\pi} \mathcal{G}_0(p_x, p_{1y}, E)\right] = 0, \qquad (15)$$

with $\mathcal{G}_0(p_x, p_{1y}, E)$ being the unperturbed retarded GF.

At low energies we can use the approximation

$$\mathcal{H}_{\boldsymbol{p}}^{\rm 2D} \approx \begin{pmatrix} \xi_p & i\varkappa(p_x + ip_y) \\ -i\varkappa(p_x - ip_y) & -\xi_p \end{pmatrix}, \qquad (16)$$

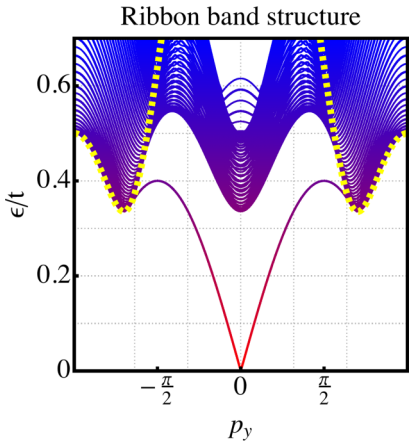

FIG. 5. The band structure of a 2D infinite ribbon obtained via numerical diagonalization of the tight-binding Hamiltonian. We note the formation of chiral dispersive Majorana modes with energies $E_\pm = \pm\varkappa p_y$, as expected theoretically for a 2D p-wave superconductor. Parameters are the same as in Fig. 4, and the width of the ribbon is 101 sites. The infinite system (bulk) spectrum is denoted by the dashed yellow lines.

where $\xi_{\boldsymbol{p}} \equiv \frac{\boldsymbol{p}^2}{2m_0} - \frac{p_F^2}{2m_0}$, with p_F denoting the Fermi momentum, m_0 the quasiparticle mass, and $\varkappa$ the p-wave pairing parameter. Such a low-energy description enables us to obtain in the limit of $U \to \infty$ an exact analytical solution of the Eq. (15) for the poles of the T-matrix,

$$E_\pm = \pm\varkappa p_y. \tag{17}$$

We note that when $p_y \to 0$, $E \to 0$, which is consistent with previous findings. These two solutions correspond to counterpropagating chiral Majorana modes.

To obtain information about the higher-energy bound states we plot the average perturbed spectral function $A(\boldsymbol{p}, E) = -\frac{1}{\pi}\,\mathrm{Im}\{\mathrm{tr}[\mathcal{G}(\boldsymbol{p}, \boldsymbol{p}, E)]\}$. The poles of the spectral function contain both the unperturbed band structure, as well as the impurity-induced bands. In order to obtain the energy dispersion of the bound states along the impurity direction we will take $p_x = 0$ and plot $A(0, p_y, E)$ as a function of p_y and E. In Fig. 4 we consider two values of the impurity strength $U/t = 1$ and $U/t = 100$. For a small impurity we note the formation of a finite-energy dispersive Shiba band [see Fig. 4(a)], while for the very large impurity this band touches zero at $p_y = 0$ [see Fig. 4(b)], marking the separation of the system in two independent ones and the formation of chiral Majorana states. Note here that the bands above the gap correspond to the bulk unperturbed states of the system, while the subgap band is the impurity-induced band. Note also the agreement with the low-energy approximation, where close to $p_y = 0$ the energy dispersion of the bound states is indeed described by $E_\pm = \pm\varkappa p_y$ with $\varkappa/t = 0.4$.

We compare this with a fully numerical analysis of the spectrum of a ribbon, obtained using a full tight-binding exact diagonalization via the MATQ code, and plotted in Fig. 5. We note the bulk ribbon bands (denoted in blue), quantized due to the finite size of the ribbon in the x direction. For comparison we also give the infinite-system band structure superposed as dashed yellow lines. We also note the formation of the Majorana edge states crossing at $p_y = 0$ (cf. $E_\pm = \pm\varkappa p_y$ obtained above, denoted in red). We stress the remarkable agreement between the analytical and the numerical techniques, both for the bulk, and especially for the subgap impurity states.

Our method can also help to describe more experimentally relevant situations corresponding to imperfect boundaries. We set the impurity potential to infinity, however "soft" boundaries could be described by assigning a finite value to it. We should note that even in this limit we can obtain analytically and without approximations the energies of the bound states and the form of the bound-state wave functions [see, e.g., Eqs. (9), (11), and (12)], rendering our technique very powerful from both a theoretical and experimental perspective.

Conclusions. We have developed an exact formalism, which provides us with a direct manner to describe the formation of boundary modes, as well as to calculate boundary GFs. The technique is based on modeling the boundary as a localized impurity and using the T-matrix formalism. We should point out that this formalism does not require making either a low-energy approximation, or any supplementary assumptions, and for the systems for which the form of the real-space GF can be derived analytically it does not even require a numerical integration.

We have successfully applied our method to a 1D Kitaev model and a 2D p-wave superconductor to describe the formation of Majorana states, and we have checked that our formalism is fully consistent with a tight-binding numerical approach. We note that this formalism can be generalized very easily to other models supporting end, edge, and surface states, as well as other types of bound states, regardless of their topological or trivial nature. A nonexhaustive list includes models combining s-wave superconductivity, spin-orbit coupling and a Zeeman field [29,30], surface and edge states of topological insulators [31–33], graphene [34], boundary modes of the Kane-Mele model [33], and Andreev bound states in S-N-S junctions [35], as well as Fermi-arc states in Weyl and Dirac semimetals [36,37]. Our results are also in agreement with previous work [38] proposing impurities as local probes of topology in band insulators. Moreover, we believe that combining scattering matrix theory and our formalism may allow one to study also arbitrary-shape potentials, thus making our proposition even more relevant from an experimental perspective; this possibility is currently under investigation.

Acknowledgments. V.K. would like to acknowledge the ERC Starting Grant No. 679722 and the Roland Gustafsson foundation for theoretical physics.

[1] *Growth, Dissolution and Pattern Formation in Geosystems*, edited by B. Jamtveit and P. Meakin (Springer, Netherlands, 1999).

[2] J. C. Slater and G. F. Koster, Phys. Rev. **94**, 1498 (1954).

[3] U. Busch and K. A. Penson, Phys. Rev. B **36**, 9271 (1987).

[4] S. Davison and M. Stęślicka, *Basic Theory of Surface States*, Monographs on the Physics and Chemistry of Materials (Clarendon, Oxford, UK, 1992).
[5] M. P. L. Sancho, J. M. L. Sancho, and J. Rubio, J. Phys. F **14**, 1205 (1984).
[6] A. Umerski, Phys. Rev. B **55**, 5266 (1997).
[7] Y. Peng, Y. Bao, and F. von Oppen, Phys. Rev. B **95**, 235143 (2017).
[8] J.-W. Rhim, J. H. Bardarson, and R.-J. Slager, Phys. Rev. B **97**, 115143 (2018).
[9] A. V. Balatsky, I. Vekhter, and J.-X. Zhu, Rev. Mod. Phys. **78**, 373 (2006).
[10] A. Y. Kitaev, Phys.-Usp. **44**, 131 (2001).
[11] G. E. Volovik, J. Exp. Theor. Phys. Lett. **70**, 609 (1999).
[12] N. Read and D. Green, Phys. Rev. B **61**, 10267 (2000).
[13] D. A. Ivanov, Phys. Rev. Lett. **86**, 268 (2001).
[14] G. D. Mahan, *Many-Particle Physics* (Springer, New York, 2000).
[15] J. M. Byers, M. E. Flatté, and D. J. Scalapino, Phys. Rev. Lett. **71**, 3363 (1993).
[16] W. Ziegler, D. Poilblanc, R. Preuss, W. Hanke, and D. J. Scalapino, Phys. Rev. B **53**, 8704 (1996).
[17] M. I. Salkola, A. V. Balatsky, and D. J. Scalapino, Phys. Rev. Lett. **77**, 1841 (1996).
[18] C. Bena, Phys. Rev. Lett. **100**, 076601 (2008).
[19] L. Yu, Acta Phys. Sin. **21**, 75 (1965).
[20] H. Shiba, Prog. Theor. Phys. **40**, 435 (1968).
[21] A. I. Rusinov, Sov. J. Exp. Theor. Phys. Lett. **9**, 85 (1969).
[22] F. Pientka, L. I. Glazman, and F. von Oppen, Phys. Rev. B **88**, 155420 (2013).
[23] V. Kaladzhyan, C. Bena, and P. Simon, Phys. Rev. B **93**, 214514 (2016).
[24] V. Kaladzhyan, C. Bena, and P. Simon, J. Phys.: Condens. Matter **28**, 485701 (2016).
[25] MATQ, www.icmm.csic.es/sanjose/MathQ/MathQ.html.
[26] D. Sticlet, C. Bena, and P. Simon, Phys. Rev. Lett. **108**, 096802 (2012).
[27] N. Sedlmayr and C. Bena, Phys. Rev. B **92**, 115115 (2015).
[28] See Supplemental Material at http://link.aps.org/supplemental/10.1103/PhysRevB.100.081106 for T-matrix behavior at the phase transition of a 1D Kitaev chain.
[29] Y. Oreg, G. Refael, and F. von Oppen, Phys. Rev. Lett. **105**, 177002 (2010).
[30] R. M. Lutchyn, J. D. Sau, and S. Das Sarma, Phys. Rev. Lett. **105**, 077001 (2010).
[31] L. Fu and C. L. Kane, Phys. Rev. Lett. **100**, 096407 (2008).
[32] X.-L. Qi and S.-C. Zhang, Rev. Mod. Phys. **83**, 1057 (2011).
[33] S. Pinon, V. Kaladzhyan, and C. Bena, arXiv:1906.08268.
[34] W. Yao, S. A. Yang, and Q. Niu, Phys. Rev. Lett. **102**, 096801 (2009).
[35] S. Pinon, V. Kaladzhyan, and C. Bena, arXiv:1906.10139.
[36] X. Wan, A. M. Turner, A. Vishwanath, and S. Y. Savrasov, Phys. Rev. B **83**, 205101 (2011).
[37] R. Okugawa and S. Murakami, Phys. Rev. B **89**, 235315 (2014).
[38] R.-J. Slager, L. Rademaker, J. Zaanen, and L. Balents, Phys. Rev. B **92**, 085126 (2015).